

Supporting Information

Edge-directed [(M₂)₂L₄] Tetragonal Metal-Organic Polyhedra Decorated Using a Square Paddle-wheel Secondary Building Unit

M. Jaya Prakash,^a Minhak Oh,^a Xinfang Liu,^a Kwi Nam Han,^a Gi Hun Seong^a and Myoung Soo Lah^{*a}

^a Department of Chemistry and Applied Chemistry, College of Science and Technology, Hanyang University, Ansan, Kyunggi-Do 426-791, Korea. Fax: 82 31 436 8100; Tel: 82 31 400 5496
E-mail: mslah@hanyang.ac.kr

Materials

The following chemicals were used as received with no further purification: methyl-3-iodobenzoate, methyl-3-iodo-4-methoxybenzoate, diethylamine, copper(I) iodide, 1,3-diethynylbenzene, dichlorobis(triphenylphosphine)palladium(II), and $\text{Cu}(\text{NO}_3)_2 \cdot 3\text{H}_2\text{O}$ from Sigma-Aldrich, Inc.; *N, N'*-dimethylformamide (DMF), acetonitrile, methanol, and methylene chloride (MC) from Junsei and 1 M HCl solution.

General procedures

Infrared spectra were recorded, using KBr pellets, in the range 4000–400 cm^{-1} using a Varian FTS 1000 FT-IR spectrometer. Nuclear magnetic resonance (NMR) spectra were recorded on Varian-300 and Varian-500 NMR spectrometers. Mass spectral data were obtained on a Jeol JMS 700 high-resolution mass spectrometer at the Korea Basic Science Institute (Daegu). Powder X-ray diffraction (PXRD) data were obtained using a Rigaku D/Max 2500/PC automated diffractometer. Atomic force microscopy (AFM) images were recorded in tapping mode using a Multimode Nanoscope IV (Digital Instrument, Veeco Metrology Group, Santa Barbara, CA, USA) using etched silicon probes. Images were recorded in height mode, and Nanoscope IV software was used for data processing.

Ligand synthesis

Preparation of 3,3'-[1,3-benzenediyl-di(ethynyl)]dibenzoic acid dimethyl ester: A 2.61 g (10.1 mmol) sample of methyl-3-iodobenzoate was dissolved in 120 mL of diethylamine in an inert atmosphere. To this solution, a 0.100 g (0.142 mmol) sample of dichlorobis(triphenylphosphine)palladium(II) and a 0.200 g (0.105 mmol) sample of copper(I) iodide were added, and the mixture was stirred for 30 minutes. A 0.680 mL (5.23 mmol) sample of 1,3-diethynylbenzene was added dropwise to the reaction mixture through the funnel, and the mixture was stirred for 48 h at an ambient temperature. The solvent was evaporated, and the residue was dissolved in 50 mL of methylene chloride, and hydrophilic materials were removed using 100 mL of H_2O extraction seven times. The organic layer was dried with anhydrous magnesium sulfate, and the solvent was evaporated. The crude product in 100 mL MeOH was crushed to small pieces using a

spatula and stirred for 3–4 h. The solid product was filtered using a frit [light yellow powder, yield = 1.57 g (79.7%)]. IR (KBr): ν/cm^{-1} : 3422, 2960, 1717, 1598, 1482, 1440, 1290, 1260, 1160, 972, 920, 799, 753, 681. $^1\text{H-NMR}$ (CDCl_3 -*d*, δ/ppm): 8.22 (t, 2H, ArH), 8.02 (t, 2H, ArH), 7.73 (m, 2H, ArH), 7.71 (t, 1H, ArH), 7.54 (d, 1H, ArH), 7.51 (d, 2H, ArH), 7.43 (m, 2H, ArH), 3.95 (s, 6H, CH). $^{13}\text{C-NMR}$ (CDCl_3 -*d*, δ/ppm): 166.60, 135.94, 134.91, 133.02, 131.81, 130.66, 129.64, 128.78, 123.61, 123.48, 89.50, 89.18, 52.56.

Preparation of 3,3'-[1,3-benzenediyl-di(ethynyl)]dibenzoic acid (H_2L^1): A 1.30 g (3.29 mmol) sample of 3,3'-[1,3-benzenediyl-di(ethynyl)]dibenzoic acid dimethyl ester in 30 mL MeOH was slowly added to the solution of a 3.96 g (70.7 mmol) sample of KOH dissolved in 100 mL MeOH in a 250-mL round-bottomed flask. The solution was heated to 70 °C and stirred for 5 h. The solvent was evaporated, and the residue was redissolved in 100 mL of H_2O . The pH of the solution was adjusted to 2–3 using 1 M HCl solution, and the mixture was stirred for an additional 2–3 h. The precipitate was filtered using a frit and dried at 45 °C in an oven [white powder, yield = 1.16 g, (96.6%)]. IR (KBr): ν/cm^{-1} : 3000, 2887, 2660, 1485, 1449, 1316, 1165, 912, 790, 754, 679, 532. $^1\text{H-NMR}$ ($\text{DMSO-}d_6$, δ/ppm): 13.00 (s, 2H, COOH), 8.10 (t, 1H, ArH), 7.99 (d, 2H, ArH), 7.82 (d, 2H, ArH), 7.79 (s, 1H, ArH), 7.66 (t, 1H, ArH), 7.63 (d, 2H, ArH), 7.54 (m, 2H, ArH). $^{13}\text{C-NMR}$ ($\text{DMSO-}d_6$, δ/ppm): 167.28, 135.91, 134.93, 132.81, 132.62, 132.51, 130.34, 130.10, 129.91, 123.36, 123.00, 89.89, 89.62. ESI-HRMS $m/z = 366.0895$ [$\text{H}_2\text{L}^1 + \text{H}^+$] (calcd. 366.0892).

Preparation of 3,3'-[1,3-benzenediyl-di(ethynyl)]bis(4-methoxy)benzoic acid dimethyl ester: A 3.0 g (10.2 mmol) sample of methyl-3-iodo-4-methoxybenzoate was dissolved in 120 mL of diethylamine in an inert atmosphere. To this solution a 0.100 g (0.142 mmol) sample of dichlorobis(triphenylphosphine)palladium(II) and a 0.200 g (0.105 mmol) sample of copper(I) iodide were added, and the mixture was stirred for 30 min. A 0.680 mL (5.23 mmol) sample of 1,3-diethynylbenzene was added drop-wise to the reaction mixture through the funnel and stirred for 48 h at an ambient temperature. The solvent was evaporated, the residue was dissolved in 50 mL of methylene chloride, and hydrophilic materials were removed using 100 mL of H_2O extraction seven times. The organic layer was dried with anhydrous magnesium sulfate, and the solvent was

evaporated. The crude product in 100 mL MeOH was crushed to small pieces using a spatula and stirred for 3–4 h. The solid product was filtered using a frit [light yellow powder, yield = 1.85 g (81.5%)]. IR (KBr, v/cm^{-1}): 3445, 2950, 2940, 1719, 1602, 1591, 1503, 1437, 1314, 1264, 1238, 1185, 1119, 1024, 988, 825, 789, 764, 728, 680, 635, 528, 462. ^1H -NMR (CDCl_3 -*d*, δ/ppm): 8.20 (d, 2H, ArH), 8.02 (dd, 2H, ArH), 7.77 (s, 1H, ArH), 7.52 (dd, 2H, ArH), 7.35 (t, 1H, ArH), 6.94 (d, 2H, ArH), 3.98 (s, 6H, CH), 3.91 (s, 6H, CH). ^{13}C -NMR (CDCl_3 -*d*, δ/ppm): 166.41, 163.52, 135.42, 134.97, 131.99, 131.69, 128.61, 123.71, 122.78, 112.62, 110.40, 93.33, 85.50, 56.35, 52.26. ESI-HRMS: m/z = 454.1420 (calcd. 454.1416).

Preparation of 3,3'-[1,3-benzenediyl]di(ethynyl)bis(4-methoxy)benzoic acid (H_2L^2): A 1.62 g (3.34 mmol) sample of 3,3'-[1,3-benzenediyl]di(ethynyl)bis(4-methoxy)benzoic acid dimethyl ester in 30 mL MeOH was slowly added to the solution of a 3.96 g (70.7 mmol) sample of KOH dissolved in 100 mL MeOH in a 250-mL round-bottomed flask. The solution was heated to 70 °C and stirred for 5 h. The solvent was evaporated, and the residue was redissolved in 100 mL of H_2O . The pH of the solution was adjusted to 2–3 using 1 M HCl solution, and the mixture was stirred for an additional 2–3 h. The precipitate was filtered using a frit and dried at 45 °C in an oven [white powder, yield = 1.15 g, (75.6%)]. IR (KBr, v/cm^{-1}): 3432, 2840, 1686, 1601, 1592, 1501, 1438, 1398, 1315, 1265, 1181, 1021, 915, 826, 793, 769, 685, 630, 538, 511. ^1H -NMR ($\text{DMSO-}d_6$, δ/ppm): 12.90 (s, 2H, COOH), 8.04 (s, 2H, ArH), 7.98 (d, 2H, ArH), 7.71 (s, 1H, ArH), 7.60 (d, 2H, ArH), 7.48 (t, 1H, ArH), 7.22 (d, 2H, ArH), 3.95 (s, 6H, CH). ^{13}C -NMR ($\text{DMSO-}d_6$, δ/ppm): 166.34, 162.93, 134.42, 133.84, 132.18, 131.58, 129.46, 123.09, 123.03, 111.42, 111.09, 92.38, 85.92, 56.35. ESI-HRMS: m/z = 426.1106 [$\text{H}_2\text{L}^2 + \text{H}^+$] (calcd. 426.1103).

Synthesis of metal-organic polyhedra

Preparation of MOP-1a and MOP-1b: A solution of a 18.3 mg (0.0499 mmol) sample of H_2L^1 and 46.5 mg (0.192 mmol) $\text{Cu}(\text{NO}_3)_2 \cdot 3\text{H}_2\text{O}$ was prepared in 5 mL of DMF and placed in a glass tube, which was then sealed and heated to 85 °C in an oven. After 4 days, crystals with two slightly different morphologies were formed. The crystals were soaked in DMF overnight, filtered, and separated manually under an optical microscope. The

major form of the crystals (~80%) were block shaped and light greenish-blue colored (MOP-1a), and the minor form of the crystals (~20%) is rectangle shaped and dark-blue colored (MOP-1b) (Figure S1). The overall yield = 24.4 mg (9.5%).

MOP-1a: IR (KBr, cm^{-1}): 3647, 3430, 1619, 1597, 1573, 1434, 1397, 803, 762, 704, 683, 501. Elemental analysis: Calcd. for $[\text{Cu}_4\text{L}^1_4(\text{DMF})_4] \cdot (\text{DMF})_3(\text{H}_2\text{O})_3$ ($\text{C}_{117}\text{H}_{103}\text{N}_7\text{O}_{26}\text{Cu}_4$, fw = 2277.32): C 61.71, H 4.56, N, 4.31%. Found: C 61.66, H 4.30, N 4.30%.

MOP-1b: IR (KBr, cm^{-1}): 3420, 2928, 1663, 1627, 1597, 1572, 1431, 1396, 1097, 804, 766, 703, 684, 490. Elemental analysis: Calcd. for $[\text{Cu}_4\text{L}^1_4(\text{DMF})_4] \cdot (\text{DMF})_5(\text{H}_2\text{O})_5$ ($\text{C}_{123}\text{H}_{121}\text{N}_9\text{O}_{30}\text{Cu}_4$, fw = 2459.54): C 60.07, H 4.96, N 5.13%. Found: C 60.20, H 4.65, N 5.30%.

Preparation of MOP-2: A solution of a 21.3 mg (0.0499 mmol) sample of H_2L^2 and 46.5 mg (0.192 mmol) $\text{Cu}(\text{NO}_3)_2 \cdot 3\text{H}_2\text{O}$ was prepared in 5 mL of DMF + CH_3CN (1:1) solvent mixture and placed in a glass tube, which was then sealed and heated to 85 °C in an oven. After 4 days, blue, block shaped crystals formed and were soaked in DMF + CH_3CN (1:1) solvent mixture overnight, filtered, and air-dried. Yield = 28.5 mg (9.7%).

MOP-2: IR (KBr, cm^{-1}): 3433, 2930, 2843, 2215, 1664, 1622, 1597, 1567, 1500, 1428, 1385, 1270, 1183, 1143, 1096, 1020, 921, 805, 780, 731, 686, 645, 539, 523, 495, 459. Elemental analysis: Calcd. for $[\text{Cu}_4\text{L}_4(\text{DMF})_4] \cdot (\text{DMF})_7(\text{H}_2\text{O})_9$ ($\text{C}_{137}\text{H}_{159}\text{N}_{11}\text{O}_{44}\text{Cu}_4$, fw = 2918): C 56.39, H 5.49, N 5.28%. Found: C 56.50, H 5.11, N 5.46%.

Crystallographic data collection and refinement of the structure

A crystal of MOP-1a was coated with paratone oil, and the diffraction data were measured at 90 K with synchrotron radiation ($\lambda = 0.72999 \text{ \AA}$) on a 4AMXW ADSC Quantum-210 detector with a Si (111) double-crystal monochromator at the Pohang Accelerator Laboratory, Korea. The diffraction data for MOP-1b and MOP-2 were measured at 99 K with synchrotron radiation ($\lambda = 0.75000 \text{ \AA}$) on a 6B MX-I ADSC Quantum-210 detector. The ADSC Quantum-210 ADX program (Ver. 1.92)^{S1} was used for data collection, and HKL2000 (Ver. 0.98.698a)^{S2} was used for cell refinement, reduction, and absorption correction.

Crystal structure of MOP-1a: A greenish-blue, block shaped crystal, $0.30 \times 0.19 \times 0.10 \text{ mm}^3$, $[\text{Cu}_4\text{L}^1_4(\text{DMF})_4]$ ($\text{C}_{114}\text{H}_{90}\text{N}_6\text{O}_{22}\text{Cu}_4$), fw = 2150.08 $\text{g} \cdot \text{mol}^{-1}$, triclinic, space group

P-1, $a = 17.475(4) \text{ \AA}$, $b = 18.723(4) \text{ \AA}$, $c = 18.786(4) \text{ \AA}$, $\alpha = 82.05(3)^\circ$, $\beta = 62.82(3)^\circ$, $\gamma = 87.67(3)^\circ$, $V = 5414.3(19) \text{ \AA}^3$, $Z = 2$, μ (synchrotron, $\lambda = 0.72999 \text{ \AA}$) = 0.847 mm^{-1} , 67,393 reflections were collected, 33,839 were unique [$R_{\text{int}} = 0.0571$]. The crystal structure was solved by direct methods and refined by full-matrix least-squares calculations with the SHELXTL-Plus software package.^{S3} Four ligand molecules, two pairs of copper ions, and four coordinated DMF and two uncoordinated DMF molecules were identified as an asymmetric unit. All nonhydrogen atoms except some atoms with high thermal anisotropies in the solvent molecules were refined anisotropically, and the hydrogen atoms were allowed to ride on their respective atoms with assigned isotropic displacement coefficients $U(\text{H}) = 1.2U(\text{C})$ or $1.5U(\text{C}_{\text{methyl}})$. The refinement converged to a final $R1 = 0.1055$ and $wR2 = 0.3436$ for 28,010 reflections of $I > 2\sigma(I)$. The structure was refined further after modification of the data for electron density of the solvent cavity including lattice solvent molecules (1116.5 \AA^3 , 20.6%) with the SQUEEZE routine of PLATON,^{S4} which led to better refinement and data convergence. Refinement of the structure converged at a final $R1 = 0.0830$ and $wR2 = 0.2427$ for 27,707 reflections with $I > 2\sigma(I)$, $R1 = 0.0911$ and $wR2 = 0.2534$ for all reflections. The largest difference peak and hole were 2.843 and $-2.362 e \cdot \text{\AA}^{-3}$ respectively.

Crystal structure of MOP-1b: A blue, block shaped crystal, $0.70 \times 0.43 \times 0.31 \text{ mm}^3$, $[\text{Cu}_2\text{L}^1_2(\text{DMF})_2]$ ($\text{C}_{54}\text{H}_{38}\text{N}_2\text{O}_{10}\text{Cu}_2$), $\text{fw} = 1001.94 \text{ g} \cdot \text{mol}^{-1}$, monoclinic, space group $C2/c$, $a = 11.245(2) \text{ \AA}$, $b = 37.235(7) \text{ \AA}$, $c = 28.875(6) \text{ \AA}$, $\beta = 98.01(3)^\circ$, $V = 11972(4) \text{ \AA}^3$, $Z = 8$, μ (synchrotron, $\lambda = 0.75000 \text{ \AA}$) = 0.766 mm^{-1} , 53,617 reflections were collected, 14,391 were unique [$R_{\text{int}} = 0.0864$]. The crystal structure was solved by direct methods and refined by full-matrix least-squares calculations with the SHELXTL-Plus software package.^{S3} Two ligand molecules, a pair of copper ions, and two coordinated DMF molecules and one-and-a-half uncoordinated DMF molecules were identified as an asymmetric unit. The central 1,3-diethynylbenzene group and one of the terminal benzene rings in one ligand were statically disordered. The geometries of the disordered benzene rings were restrained using the FLAT and the DFIX commands of SHELXTL-Plus software package. The geometries of the statically disordered coordinated DMF molecule were restrained using the FLAT command. All nonhydrogen atoms except some atoms with high thermal anisotropies in the solvent molecules were refined anisotropically, and

the hydrogen atoms were allowed to ride on their respective atoms with assigned isotropic displacement coefficients $U(H) = 1.2U(C)$ or $1.5U(C_{\text{methyl}})$. The disordered coordinated DMF molecule and the half-occupied DMF molecule were restrained during the least-squares refinement because of either poor geometry or thermal behavior. The refinement converged to a final $R1 = 0.1001$ and $wR2 = 0.2957$ for 12,035 reflections of $I > 2\sigma(I)$. The structure was refined further after modification of the data for electron density of the solvent cavity including lattice solvent molecules (3179.0 \AA^3 , 26.6%) with the SQUEEZE routine of PLATON,^{S4} which led to better refinement and data convergence. Refinement of the structure converged at a final $R1 = 0.0815$ and $wR2 = 0.2357$ for 12,173 reflections with $I > 2\sigma(I)$, $R1 = 0.0900$ and $wR2 = 0.2452$ for all reflections. The largest difference peak and hole were 1.337 and $-0.991 e\cdot\text{\AA}^{-3}$ respectively. Crystal structure of MOP-2: A blue, block shaped crystal, $0.37 \times 0.37 \times 0.30 \text{ mm}^3$, $[\text{Cu}_2\text{L}^2_2(\text{DMF})_2] \cdot 3.25\text{DMF} \cdot 2.25\text{MeCN} \cdot 0.5\text{H}_2\text{O}$ ($\text{C}_{72.25}\text{H}_{76.50}\text{N}_{7.50}\text{O}_{17.75} \text{Cu}_2$), $\text{fw} = 1460.99 \text{ g}\cdot\text{mol}^{-1}$, monoclinic, space group $P2_1/n$, $a = 13.187(3) \text{ \AA}$, $29.985(6) \text{ \AA}$, $18.713(4) \text{ \AA}$, $\beta = 93.93(3)^\circ$, $V = 7382(3) \text{ \AA}^3$, $Z = 4$, μ (synchrotron, $\lambda = 0.75000 \text{ \AA}$) = 0.648 mm^{-1} , 61,282 reflections were collected, 19,718 were unique [$R_{\text{int}} = 0.0464$]. The crystal structure was solved by direct methods and refined by full-matrix least-squares calculations with the SHELXTL-Plus software package.^{S3} Two ligand molecules, a pair of copper ions, two coordinated DMF molecules were identified as for the half of the tetragonal MOP cage in the crystallographic inversion center. Four uncoordinated DMF solvent sites with a total of 3.25 site occupancy factors, three acetonitrile sites with a total of 2.25 site occupancy factors, and a water molecule site of a half occupancy were identified as an additional asymmetric unit. All nonhydrogen atoms except some atoms with high thermal anisotropies in the solvent molecules were refined anisotropically, and the hydrogen atoms were allowed to ride on their respective atoms with assigned isotropic displacement coefficients $U(H) = 1.2U(C)$ or $1.5U(C_{\text{methyl}})$. Some C_{methyl} hydrogen atoms of the disordered solvent molecules and the water hydrogen atoms are not included in the least-squares refinement because of the poor least-square refinement convergence. The refinement converged to a final $R1 = 0.0716$ and $wR2 = 0.2019$ for 16,424 reflections of $I > 2\sigma(I)$, $R1 = 0.0829$ and $wR2 = 0.2153$ for all reflections. The largest difference peak and hole were 1.035 and $-1.256 e\cdot\text{\AA}^{-3}$ respectively.

Summary of the crystal structure refinement data are given in Tables S1–S3. CCDC 744143-744145 contain the supplementary crystallographic data of the MOP-**1a**, MOP-**1b**, and MOP-**2**. The data can be obtained free of charge at www.ccdc.cam.ac.uk/conts/retrieving.html or from the Cambridge Crystallographic Data Centre, 12, Union Road, Cambridge CB2 1EZ, UK.

References

- S1. A. J. Arvai and C. Nielsen, ADSC Quantum-210 ADX Program, Area Detector System Corporation; Poway, CA, USA, **1983**.
- S2. Z. Otwinowski and W. Minor, in *Methods in Enzymology*, ed. Carter, Jr., C. W.; Sweet, R. M. Academic Press: New York, 1997, **276**, part A, 307–326.
- S3. G. M. Sheldrick, SHELXTL-Plus, Crystal Structure Analysis Package; Bruker Analytical X-Ray: Madison, WI, USA, **1997**.
- S4. A. L. Spek, Platon program. (Ver 1.08), *Acta Crystallogr., Sect. A*, 1990, **46**, 194–201.

Table S1. Crystal data and structure refinement for MOP-1a.

Empirical formula	C ₁₁₄ H ₉₀ N ₆ O ₂₂ Cu ₄	
Formula weight	2150.08	
Temperature	90(2) K	
Wavelength	0.72999 Å	
Crystal system	Triclinic	
Space group	P-1	
Unit cell dimensions	a = 17.475(4) Å	α = 82.05(3)°
	b = 18.723(4) Å	β = 62.82(3)°
	c = 18.789(4) Å	γ = 87.67(3)°
Volume	5414.3(19) Å ³	
Z	2	
Density (calculated)	1.319 mg/m ³	
Absorption coefficient	0.847 mm ⁻¹	
F(000)	2216	
Crystal size	0.30 × 0.19 × 0.10 mm ³	
Theta range for data collection	1.35 to 31.81°	
Index ranges	-25 ≤ h ≤ 25, -26 ≤ k ≤ 26, -27 ≤ l ≤ 27	
Reflections collected	67393	
Independent reflections	33839 [R(int) = 0.0571]	
Completeness to theta = 31.81°	99.1 %	
Absorption correction	Empirical	
Max. and min. transmission	0.9201 and 0.7853	
Refinement method	Full-matrix least-squares on F ²	
Data / restraints / parameters	33839 / 8 / 1212	
Goodness-of-fit on F ²	1.086	
Final R indices [I > 2σ(I)]	R1 = 0.0830, wR2 = 0.2427	
R indices (all data)	R1 = 0.0911, wR2 = 0.2534	
Extinction coefficient	0.014(1)	
Largest diff. peak and hole	2.843 and -2.362 e·Å ⁻³	

Table S2. Crystal data and structure refinement for MOP-1b.

Empirical formula	C ₅₄ H ₃₈ N ₂ O ₁₀ Cu ₂	
Formula weight	1001.94	
Temperature	99(2) K	
Wavelength	0.75000 Å	
Crystal system	Monoclinic	
Space group	C2/c	
Unit cell dimensions	a = 11.245(2) Å	α = 90°
	b = 37.235(7) Å	β = 98.01(3)°
	c = 28.875(6) Å	γ = 90°
Volume	11972(4) Å ³	
Z	8	
Density (calculated)	1.112 Mg/m ³	
Absorption coefficient	0.760 mm ⁻¹	
F(000)	4112	
Crystal size	0.70 x 0.43 x 0.31 mm ³	
Theta range for data collection	2.01 to 30.00°	
Index ranges	-14 ≤ h ≤ 14, -49 ≤ k ≤ 49, -36 ≤ l ≤ 34	
Reflections collected	53617	
Independent reflections	14391 [R(int) = 0.0864]	
Completeness to theta = 30.00°	96.9 %	
Absorption correction	Semi-empirical from equivalents	
Max. and min. transmission	0.7986 and 0.6184	
Refinement method	Full-matrix least-squares on F ²	
Data / restraints / parameters	14391 / 47 / 754	
Goodness-of-fit on F ²	1.027	
Final R indices [I > 2σ(I)]	R1 = 0.0815, wR2 = 0.2357	
R indices (all data)	R1 = 0.0900, wR2 = 0.2452	
Extinction coefficient	0.0044(4)	
Largest diff. peak and hole	1.337 and -0.991 e·Å ⁻³	

Table S3. Crystal data and structure refinement for MOP-2.

Empirical formula	$C_{72.25}H_{76.50}N_{7.50}O_{17.75}Cu_2$	
Formula weight	1460.99	
Temperature	99(2) K	
Wavelength	0.75000 Å	
Crystal system	Monoclinic	
Space group	$P2_1/n$	
Unit cell dimensions	$a = 13.187(3)$ Å	$\alpha = 90^\circ$
	$b = 29.985(6)$ Å	$\beta = 93.93(3)^\circ$
	$c = 18.713(4)$ Å	$\gamma = 90^\circ$
Volume	$7382(3)$ Å ³	
Z	4	
Density (calculated)	1.315 Mg/m ³	
Absorption coefficient	0.648 mm ⁻¹	
F(000)	3050	
Crystal size	$0.37 \times 0.37 \times 0.30$ mm ³	
Theta range for data collection	2.06 to 31.00°	
Index ranges	$-17 \leq h \leq 17$, $-41 \leq k \leq 41$, $-25 \leq l \leq 25$	
Reflections collected	61282	
Independent reflections	19718 [R(int) = 0.0464]	
Completeness to theta = 31.00°	98.5 %	
Absorption correction	Semi-empirical from equivalents	
Max. and min. transmission	0.8293 and 0.7954	
Refinement method	Full-matrix least-squares on F ²	
Data / restraints / parameters	19718 / 6 / 983	
Goodness-of-fit on F ²	1.025	
Final R indices [I > 2σ(I)]	R1 = 0.0716, wR2 = 0.2019	
R indices (all data)	R1 = 0.0829, wR2 = 0.2153	
Largest diff. peak and hole	1.035 and -1.256 e·Å ⁻³	

Table S4. The interatomic distances (Å) in the inter-cage π - π stacking interactions observed in MOP-1a, MOP-1b, and MOP-2.

type-I	type-II	type- III
MOP-1a		
C3D ... C17D#1 3.6396(10)	C8A ... C23A#2 3.6730(12)	
C3D ... C18D#1 3.4875(9)	C9A ... C18A#2 3.4340(12)	
C3D ... C19D#1 3.7005(8)	C9A ... C19A#2 3.3747(9)	
C4D ... C19D#1 3.5196(9)	C9A ... C20A#2 3.6687(7)	
C8D ... C19D#1 3.5814(12)		
MOP-1b		
C2 ... C22#3 3.5240(8)		
C2 ... C23#3 3.6235(6)		
C3 ... C18#3 3.5237(6)		
C3 ... C22#3 3.6113(7)		
C3 ... C23#3 3.4290(7)		
C4 ... C19#3 3.5317(6)		
C4 ... C20#3 3.4748(8)		
C4 ... C21#3 3.6855(7)		
C5 ... C20#3 3.6829(6)		
C5 ... C21#3 3.6367(7)		
C8 ... C19#3 3.3671(7)		
C8 ... C20#3 3.6196(7)		
MOP-2		
C28 ... C42#4 3.6199(6)		C21 ... C22#5 3.6406(5)
C28 ... C47#4 3.5592(6)		C21 ... C23#5 3.5096(7)
C29 ... C45#4 3.5243(8)		C22 ... C22#5 3.6090(6)
C29 ... C46#4 3.5128(6)		

C30 ... C46#4 3.6268(6)

C32 ... C42#4 3.4680(6)

C32 ... C43#4 3.5179(8)

Symmetry transformations used to generate equivalent atoms: #1 2-x, 2-y, -z; #2 2-x, 1-y, -z; #3 1/2-x, 1/2-y, -z; #4 2-x, -y, -z; #5 2-x, -y, -1-z.

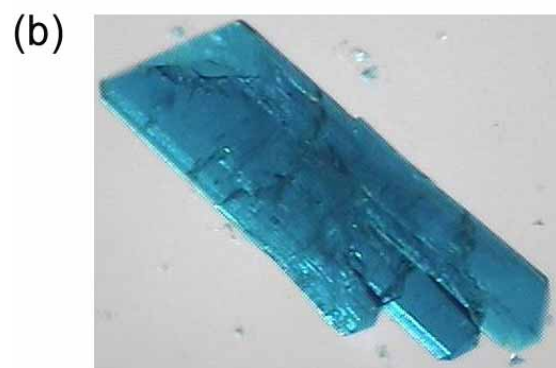
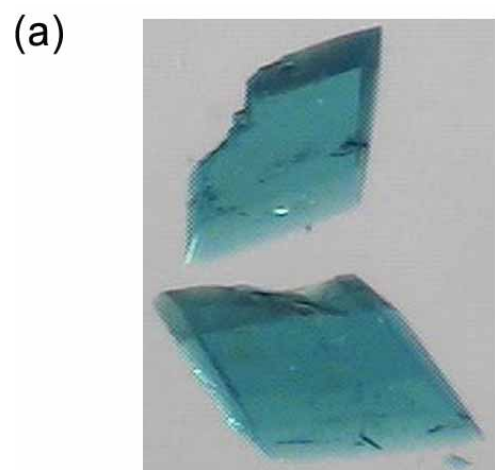


Figure S1. Photographs of (a) MOP-1a and (b) MOP-1b crystals.

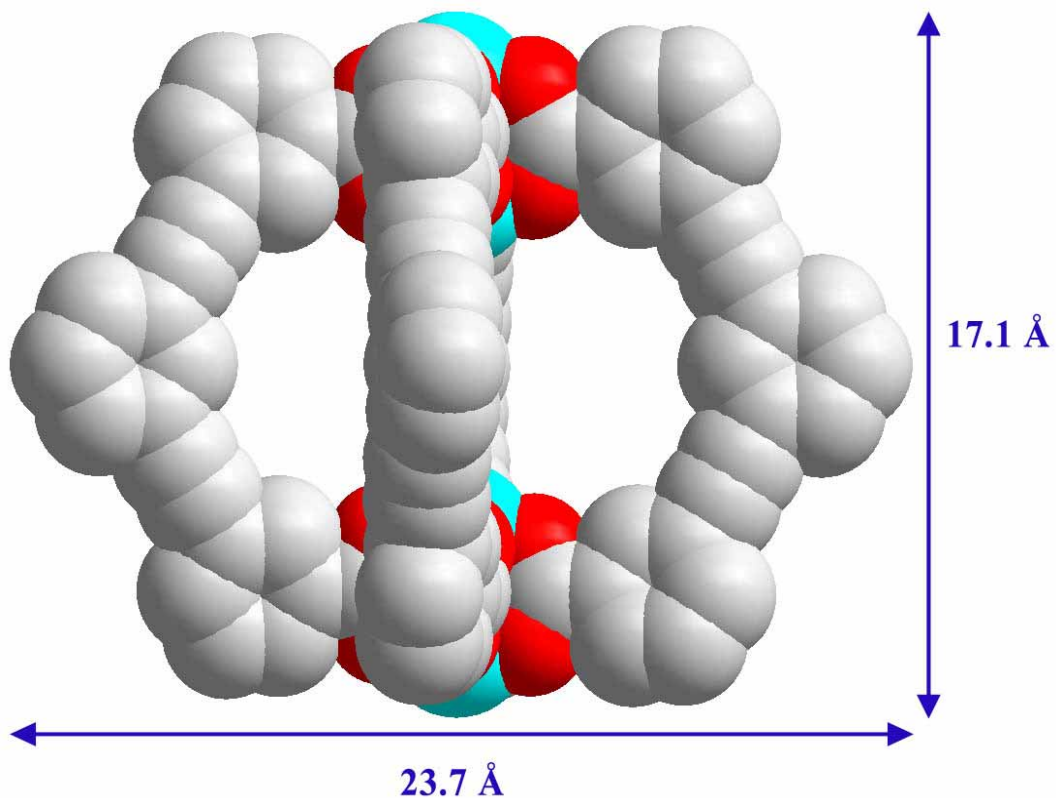


Figure S2. A CPK drawing illustrating the approximate width and height of one cage unit of MOP-1a, where solvent molecules ligated to the metal centers of the paddle-wheel units are not included.

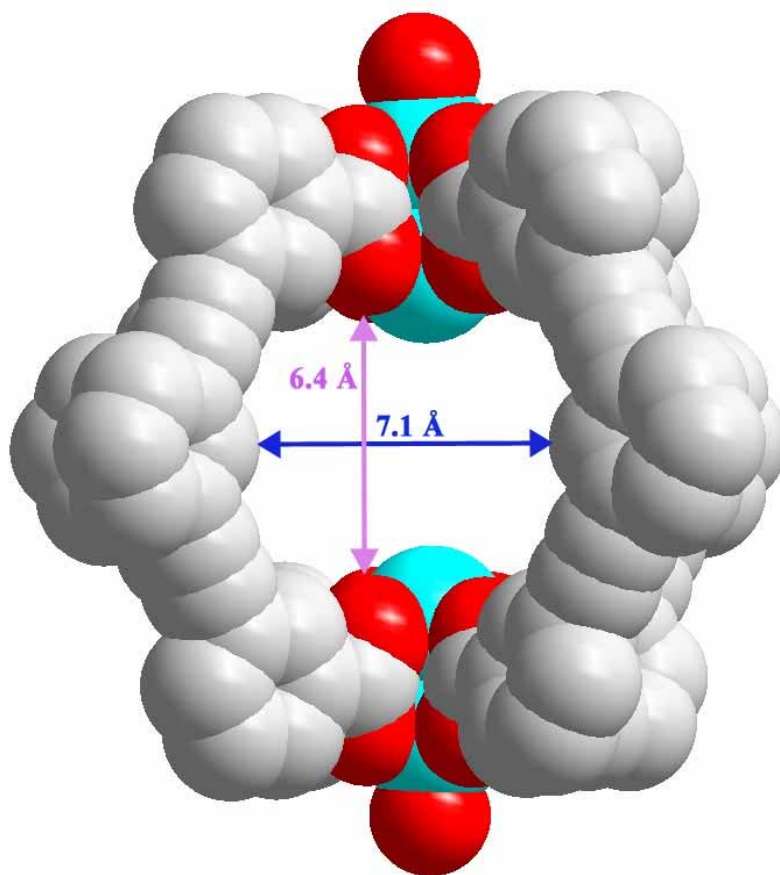


Figure S3. A CPK drawing illustrating the window dimensions of the cage in MOP-1a.

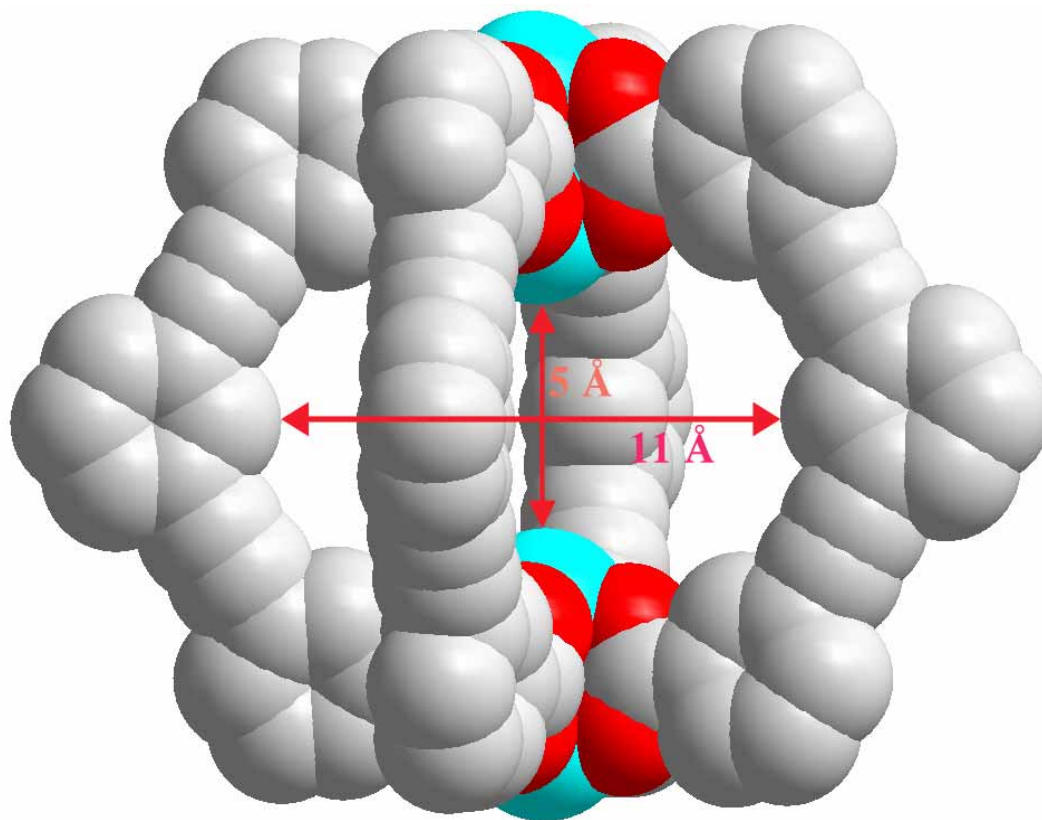


Figure S4. A CPK drawing illustrating the size of the cavity space in the cage in MOP-1a.

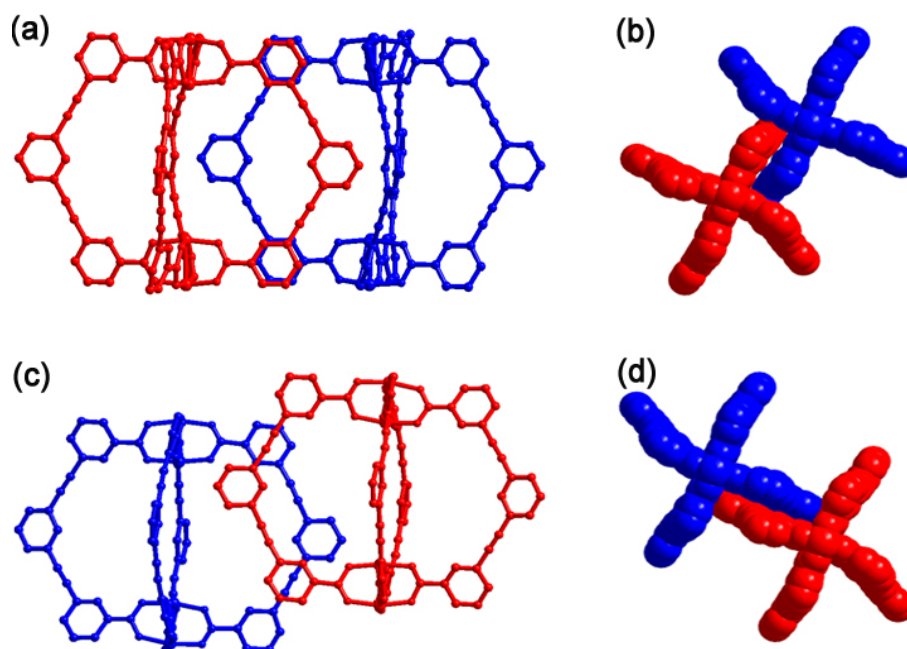


Figure S5. Ball-and-stick models of MOP-1a showing the two kinds of inter-cage π - π stacking interactions among the cages. (a) A top view of the type-I π - π stacking interactions, (b) a side view of the type-I π - π stacking interactions, (c) a top view of the type-II π - π stacking interactions, and (d) a side view the type-II π - π stacking interactions. The cages are shown with blue and red colors for clarity.

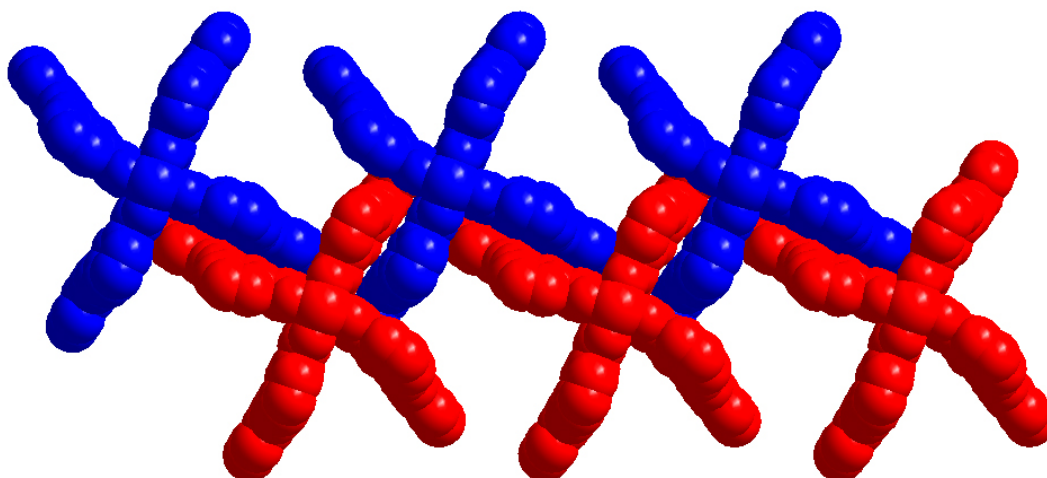


Figure S6. A CPK drawing showing of a 1D chain-like structure in MOP-**1a** formed via the two different kinds of π - π stacking interactions, type-I and type-II, among the cages. The cages are shown with blue and red colors for clarity.

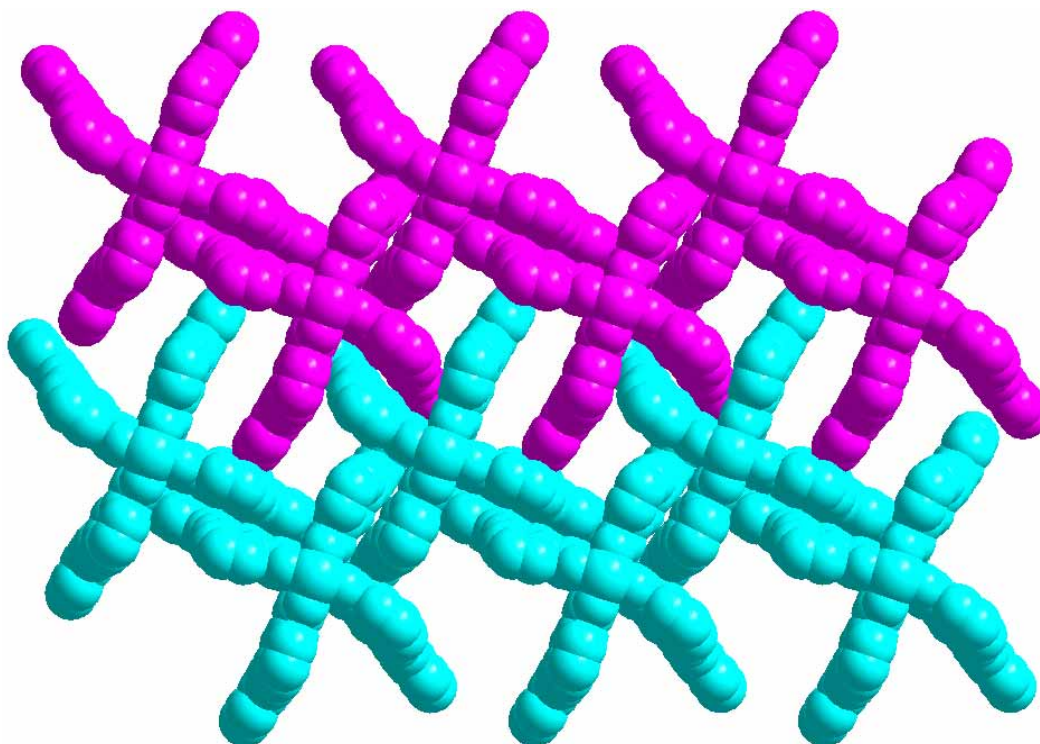


Figure S7. A CPK drawing showing a 2D sheet in MOP-**1a**, formed via only weak van der Waals interactions between the 1D chains. The 1D chains are shown with pink and cyan colors for clarity.

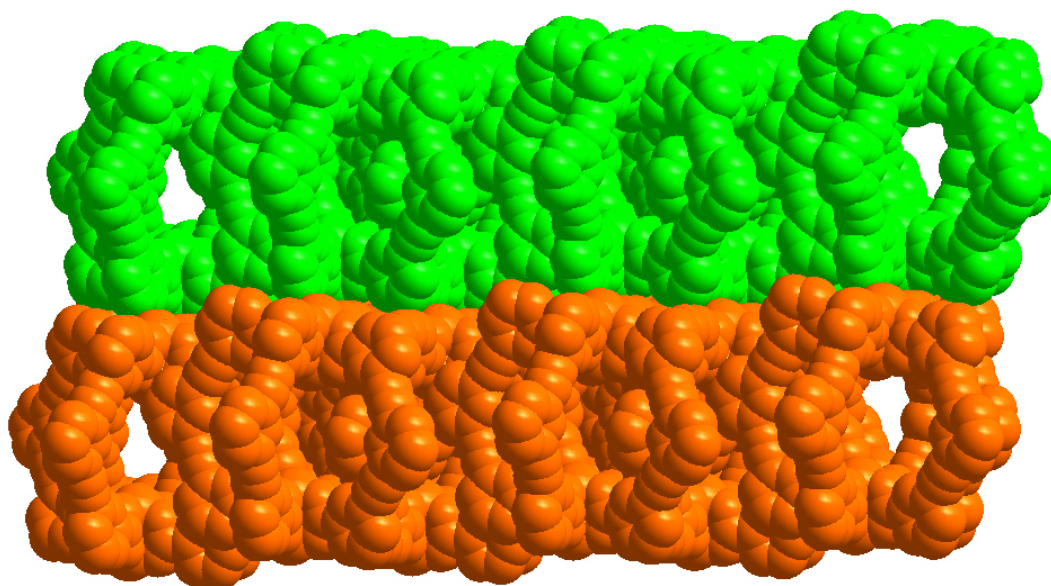


Figure S8. A CPK drawing of the crystal packing structure in MOP-1a. The extensive van der Waals interactions were observed between the 2D sheets. The two 2D sheets are shown with green and brown colors for clarity.

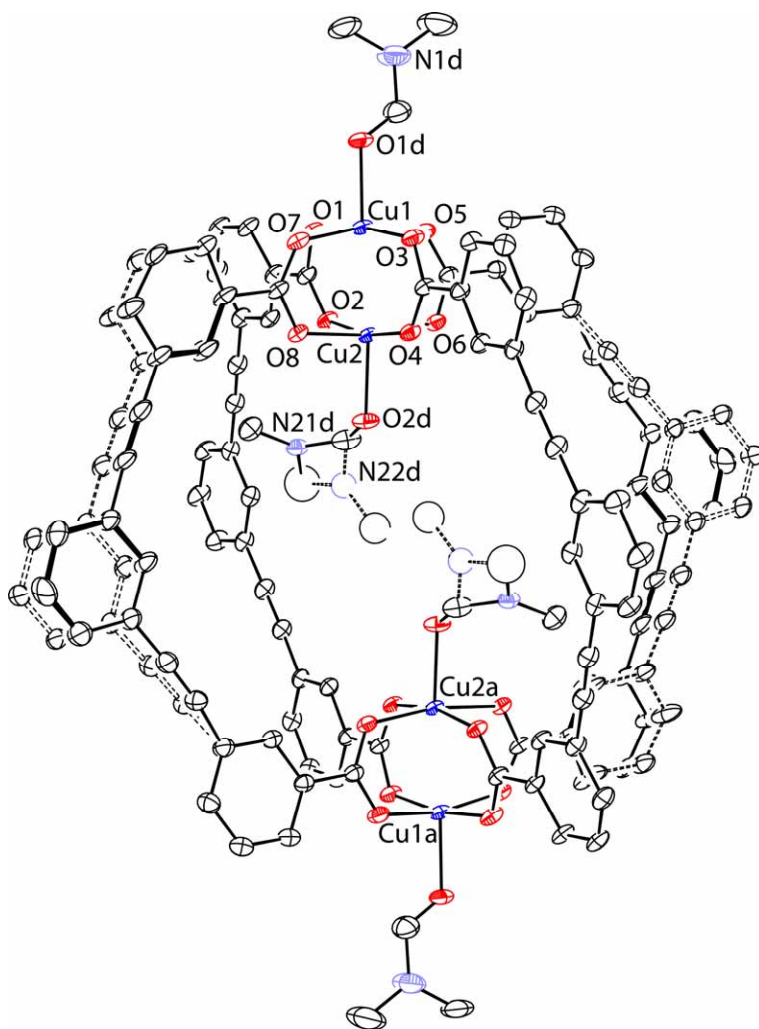


Figure S9. ORTEP representation of the one-cage unit in the crystal structure of MOP-1b with 20% of thermal ellipsoid probability displacement. Hydrogen atoms were omitted for clarity. The drawing in the dashed bonds represents the parts of the ligands and DMF molecules statically disordered in the crystal structure. Colors of atoms shown: carbon, black; nitrogen, violet; oxygen, red; and copper, blue.

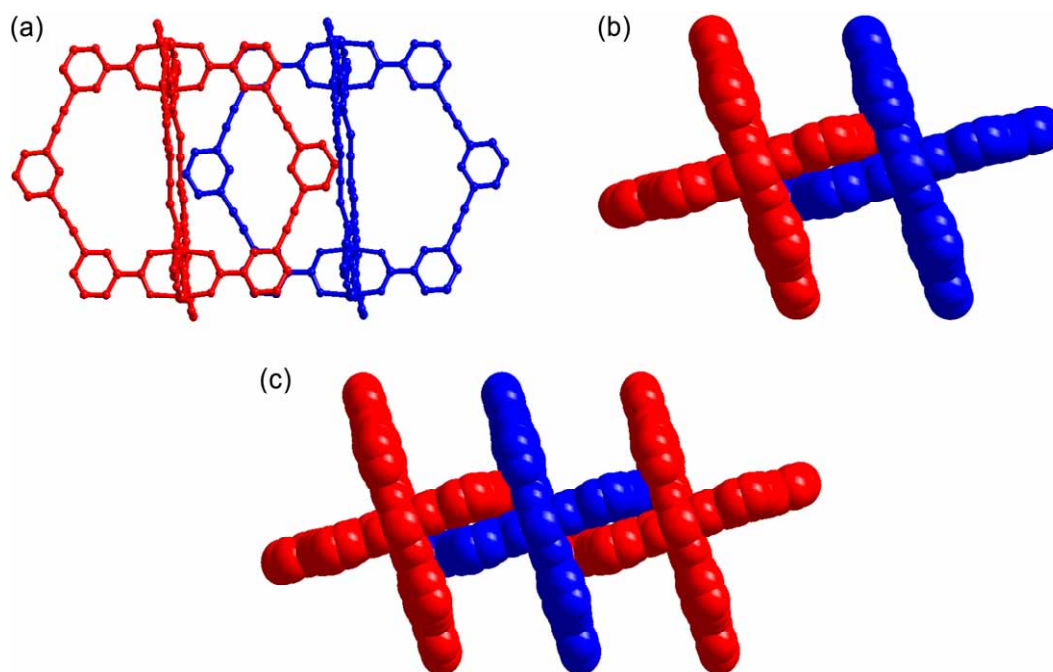


Figure S10. Ball-and-stick and CPK models of MOP-**1b** showing the type-I inter-cage π - π stacking interaction between the cages. (a) A top view and (b) a side view of the π - π stacking interactions. (c) A CPK drawing of a 1D chainlike structure in MOP-**1b** formed via the type-I π - π stacking interactions between the cages. The cages are shown with blue and red colors for clarity.

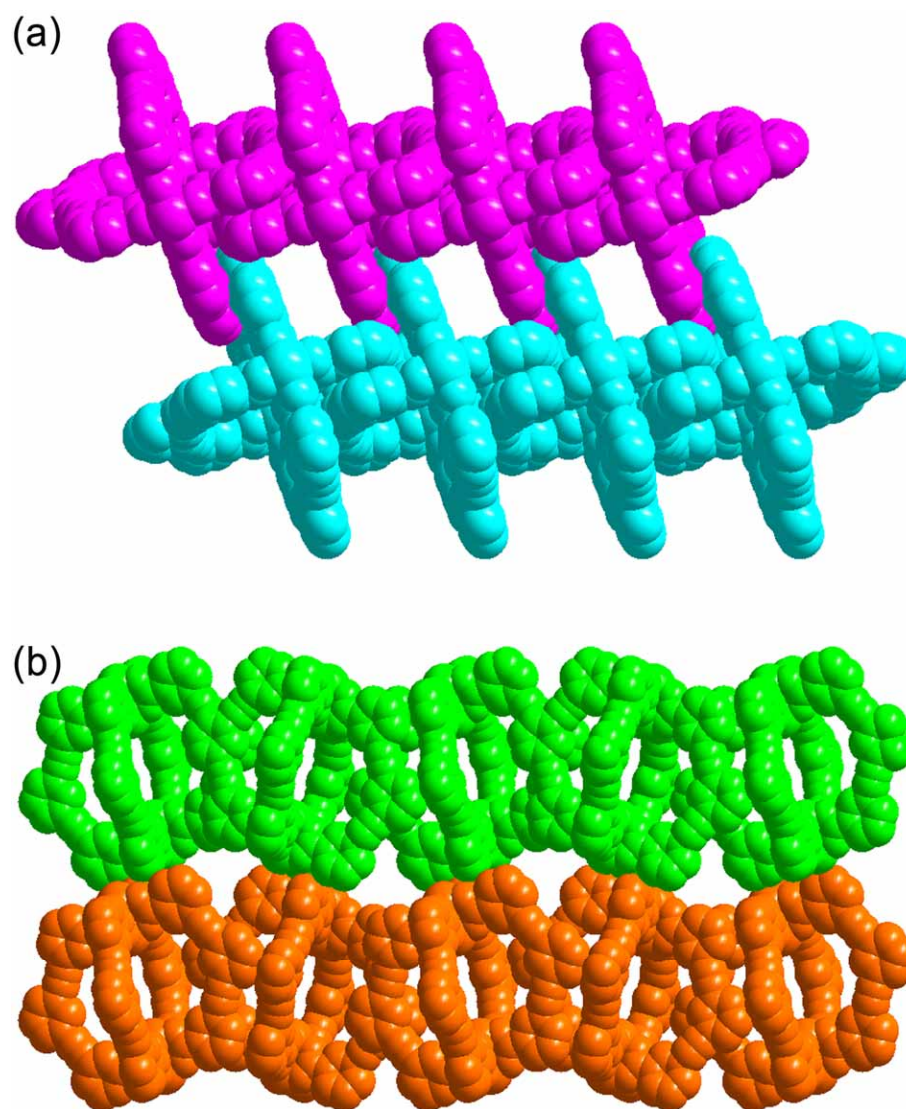


Figure S11. CPK drawings of (a) a 2D sheet structure and (b) a 3D packing structure in MOP-**1b**, where weak van der Waals interactions are the only interactions observed between the 1D chains and between the 2D sheets.

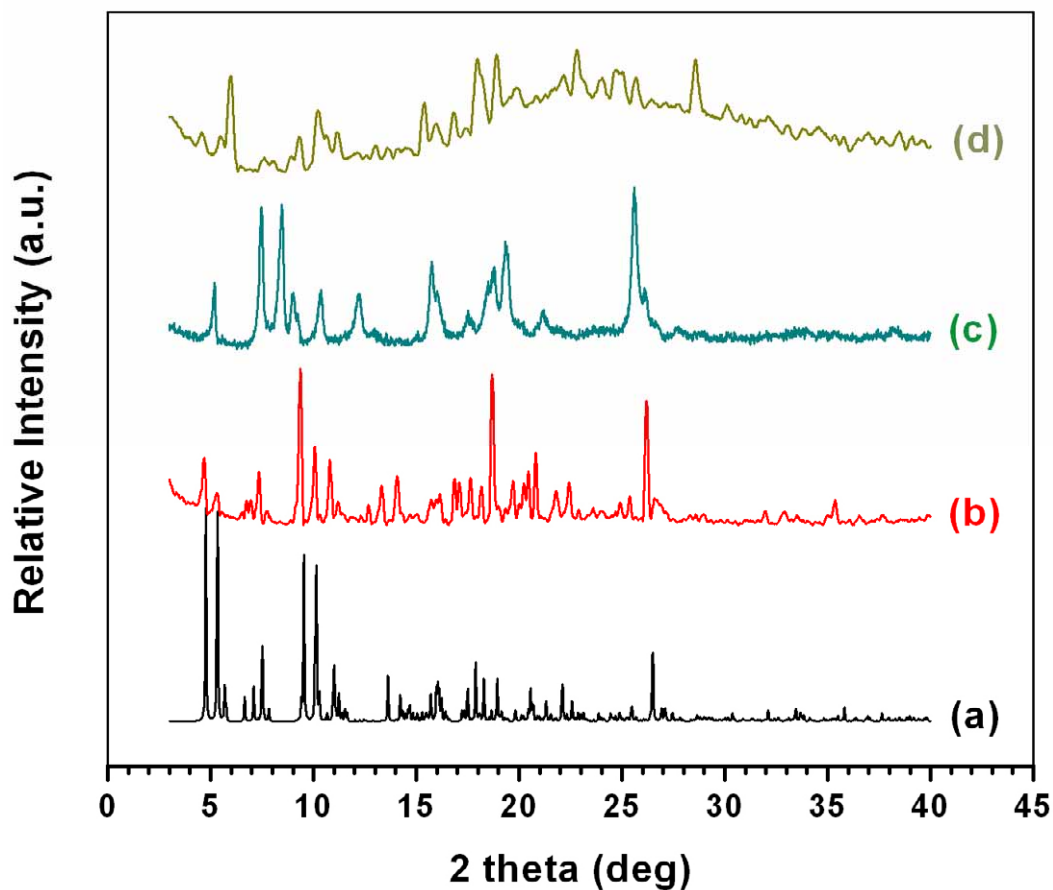


Figure S12. PXRD patterns of MOP-1a: (a) a simulation from the single-crystal structure of MOP-1a, (b) an as-synthesized sample, (c) an activated sample prepared by vacuum-drying MOP-1a at 120 °C, overnight, and (d) a sample prepared by re-soaking the activated sample in fresh DMF for 3 days.

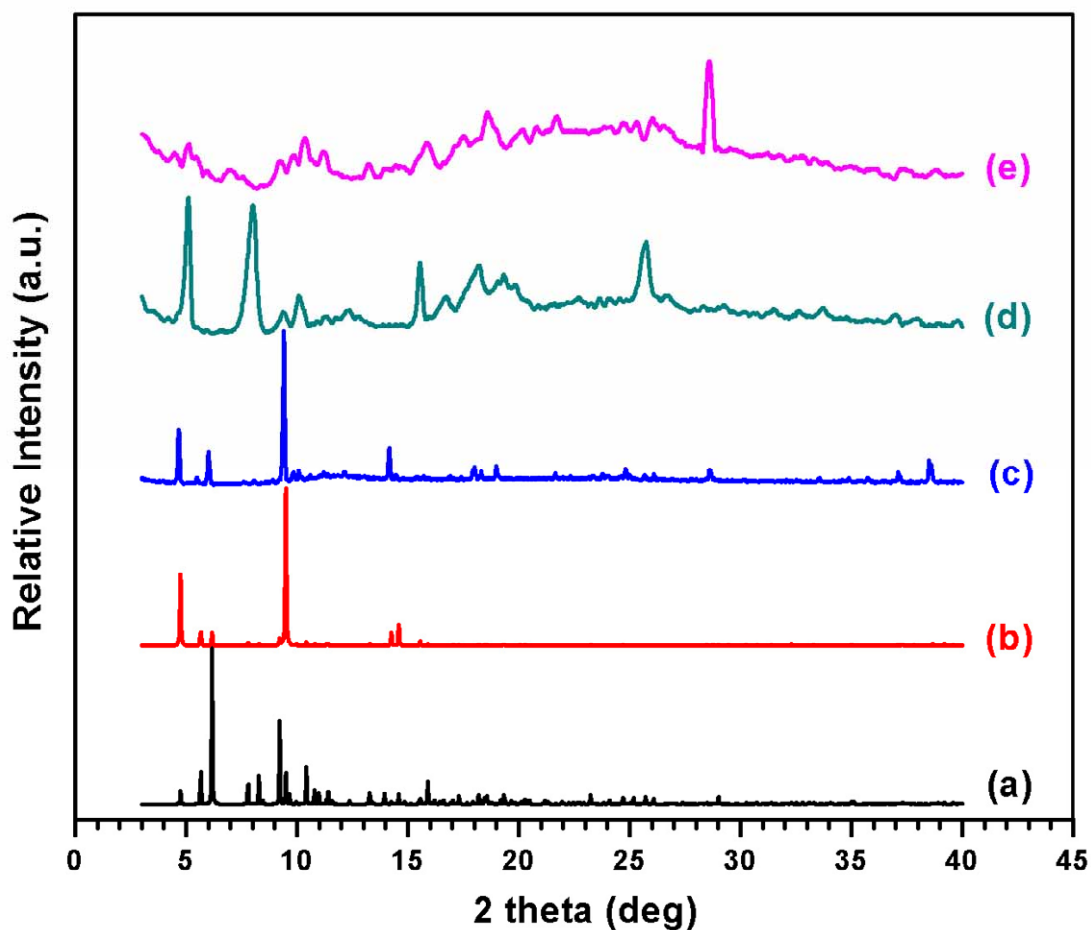


Figure S13. PXRD patterns of MOP-1b: (a) a simulation from the single-crystal structure of MOP-1b, (b) a simulated PXRD pattern with [0 1 0] preferred orientation, (c) an as-synthesized sample, (d) an activated sample prepared by vacuum-drying MOP-1b at 120 °C overnight, and (e) a sample prepared by resoaking the activated sample in fresh DMF for 3 days.

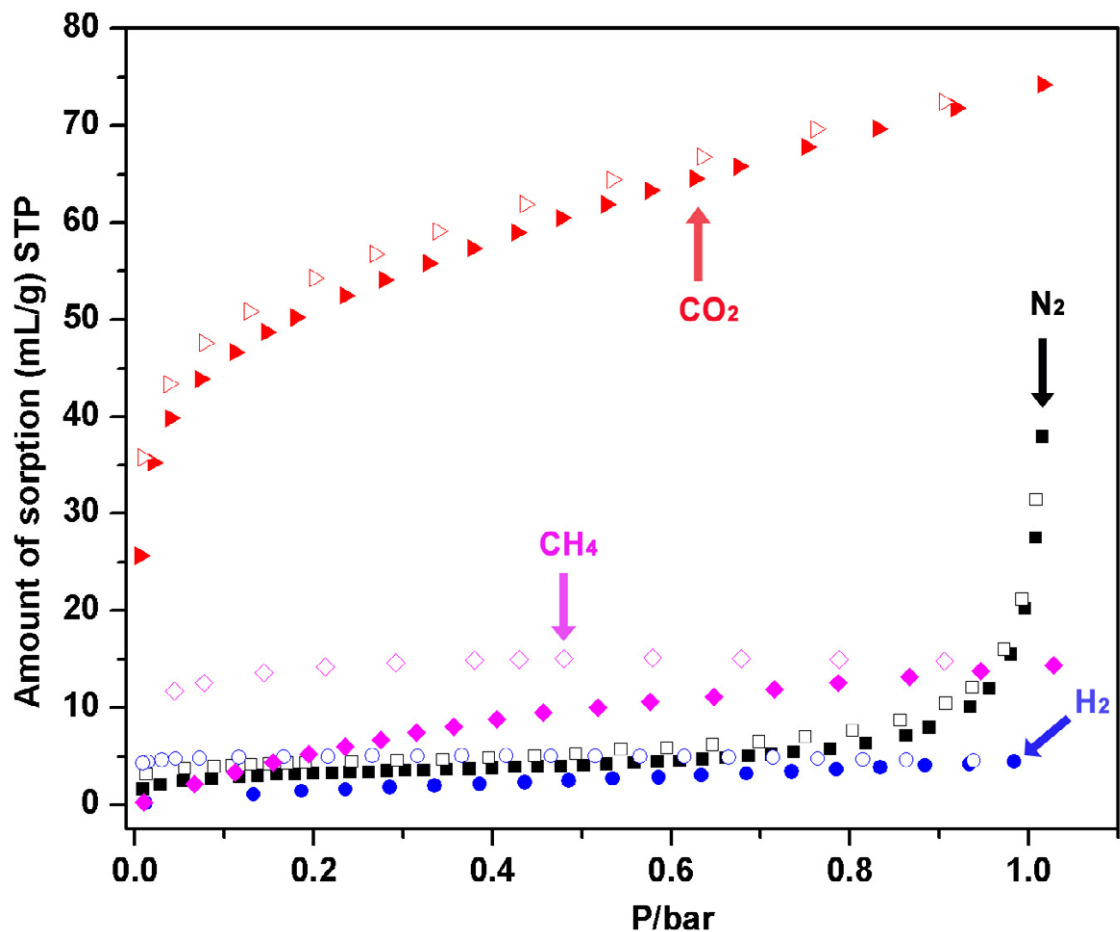


Figure S14. Gas sorption isotherms of MOP-1b. Black, N₂; pink, CH₄; blue, H₂; and red, CO₂. Filled symbols represent adsorption isotherms, and empty symbols represent desorption isotherms.

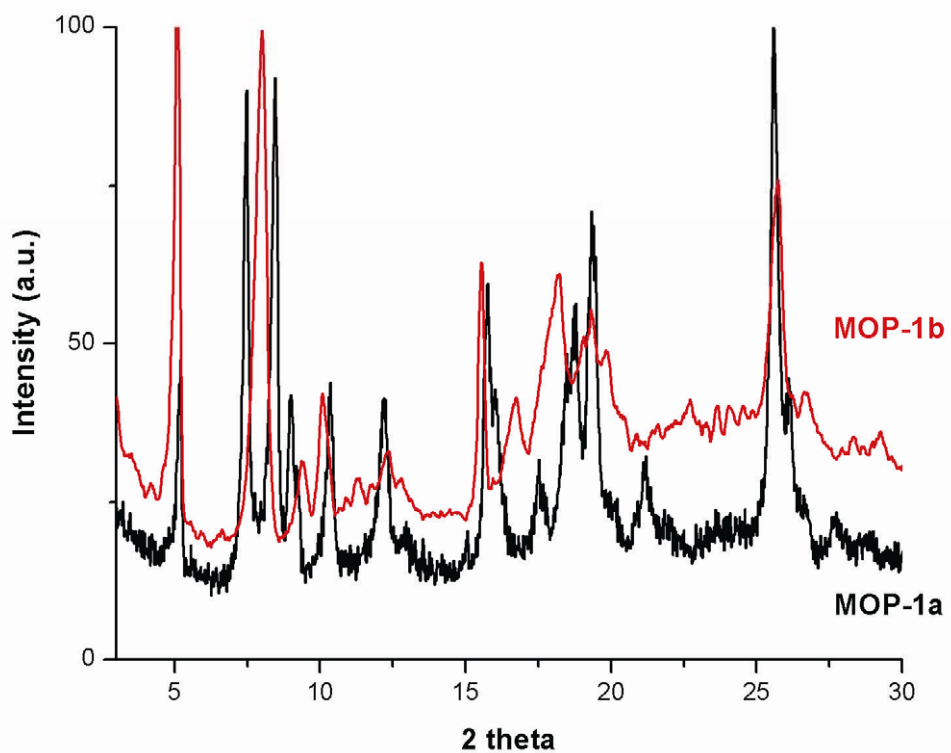


Figure S15. PXRD comparison between the activated samples of MOP-1a and MOP-1b.

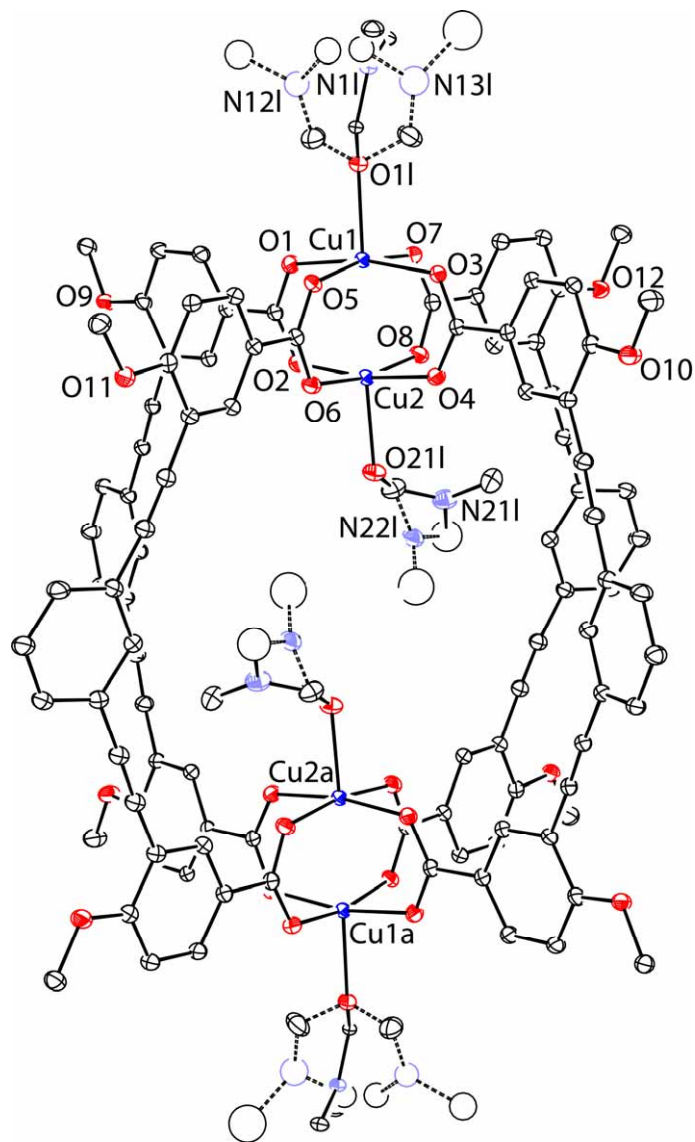


Figure S16. ORTEP representation of the one cage-unit in the crystal structure of MOP-2 with 20% of thermal ellipsoid probability displacement. Hydrogen atoms were omitted for clarity. The drawing in the dashed bonds represents the parts of the DMF molecules statically disordered in the crystal structure. Colors of atoms shown: carbon, black; nitrogen, violet; oxygen, red; and copper, blue.

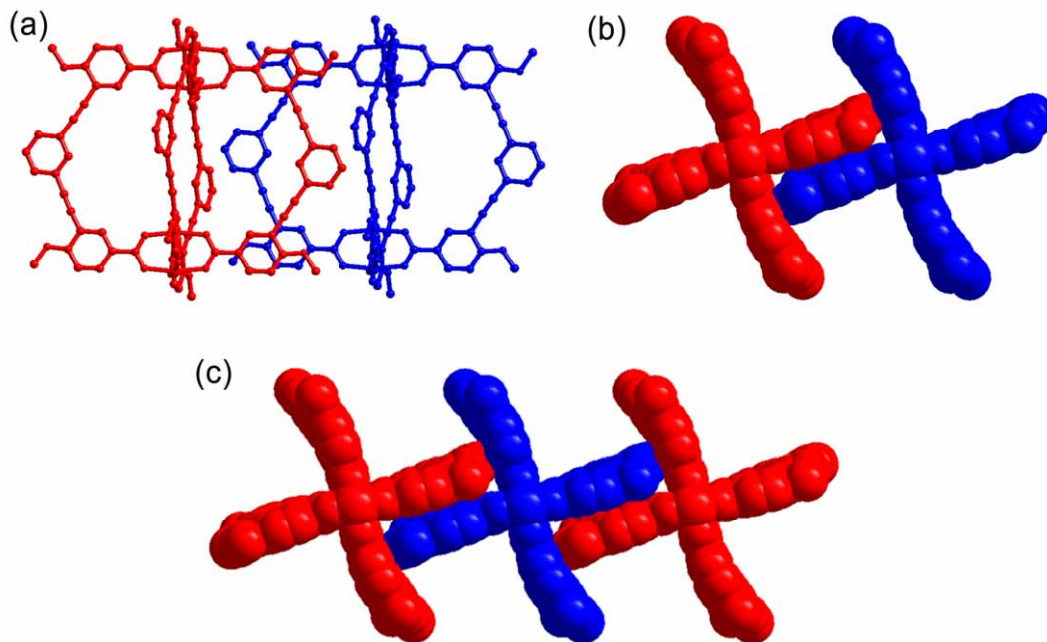


Figure S17. Ball-and-stick and CPK models of MOP-2 showing the type-I inter-cage π - π stacking interaction between the cages. (a) A top view and (b) a side view of the π - π stacking interactions. (c) A CPK drawing of a 1D chainlike structure in MOP-2 formed via the type-I π - π stacking interactions between the cages. The cages are shown with blue and red colors for clarity.

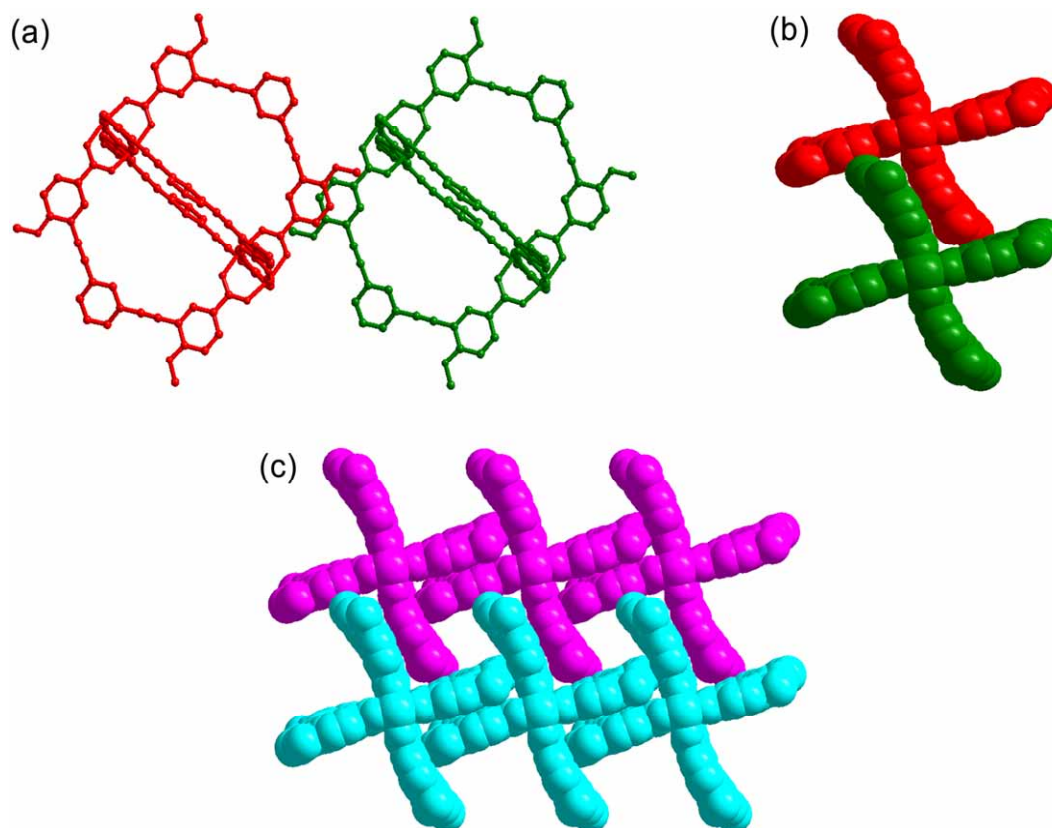


Figure S18. Ball-and-stick models of MOP-2 showing the type-III inter-cage π - π stacking interactions. (a) A top view and (b) a side view of the type-III inter-cage π - π stacking interactions. (c) A 2D sheet structure formed with the two kinds of π - π stacking interactions, type-I and type-III π - π .

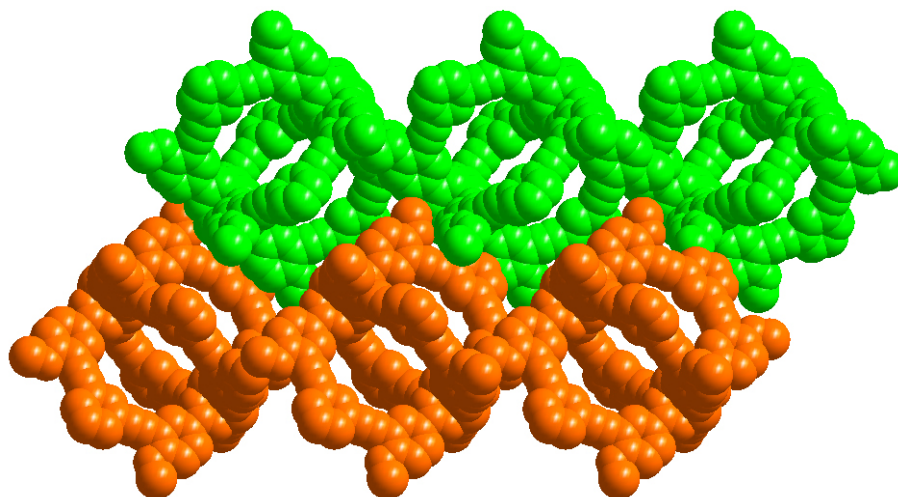


Figure S19. A ball-and-stick model of MOP-2 showing a 3D packing structure, where 2D sheets formed with two kinds of inter-cage π - π stacking interaction are stacked with weak van der Waals interactions. The layers are shown with green and brown colors for clarity.

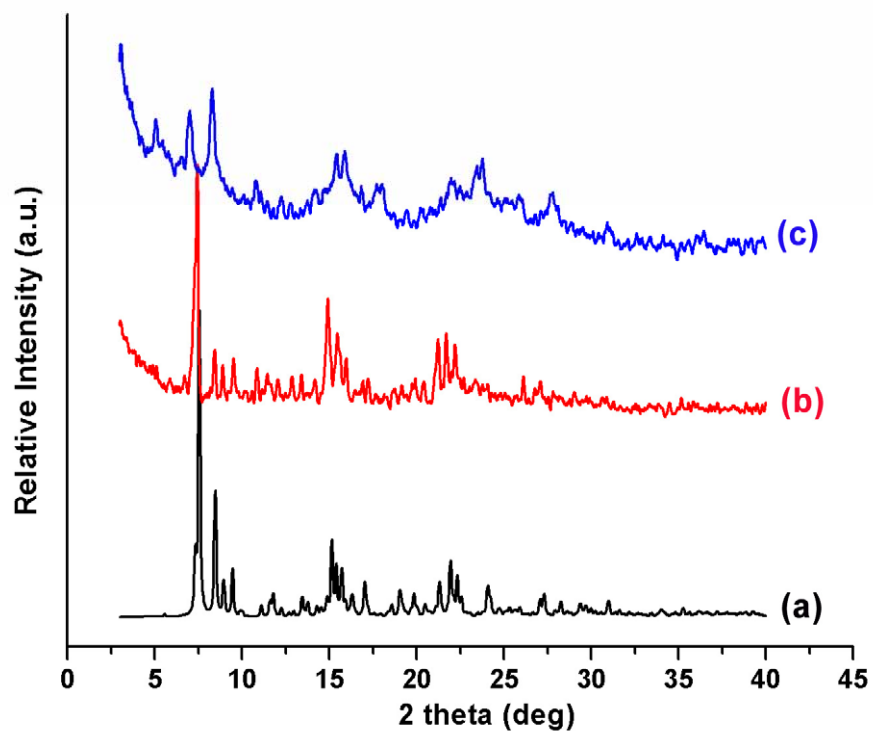


Figure S20. PXRD patterns of MOP-2: (a) a simulation from the single-crystal structure of MOP-2, (b) an as-synthesized sample, (c) an activated sample prepared by vacuum-drying MOP-2 at 120 °C, overnight.

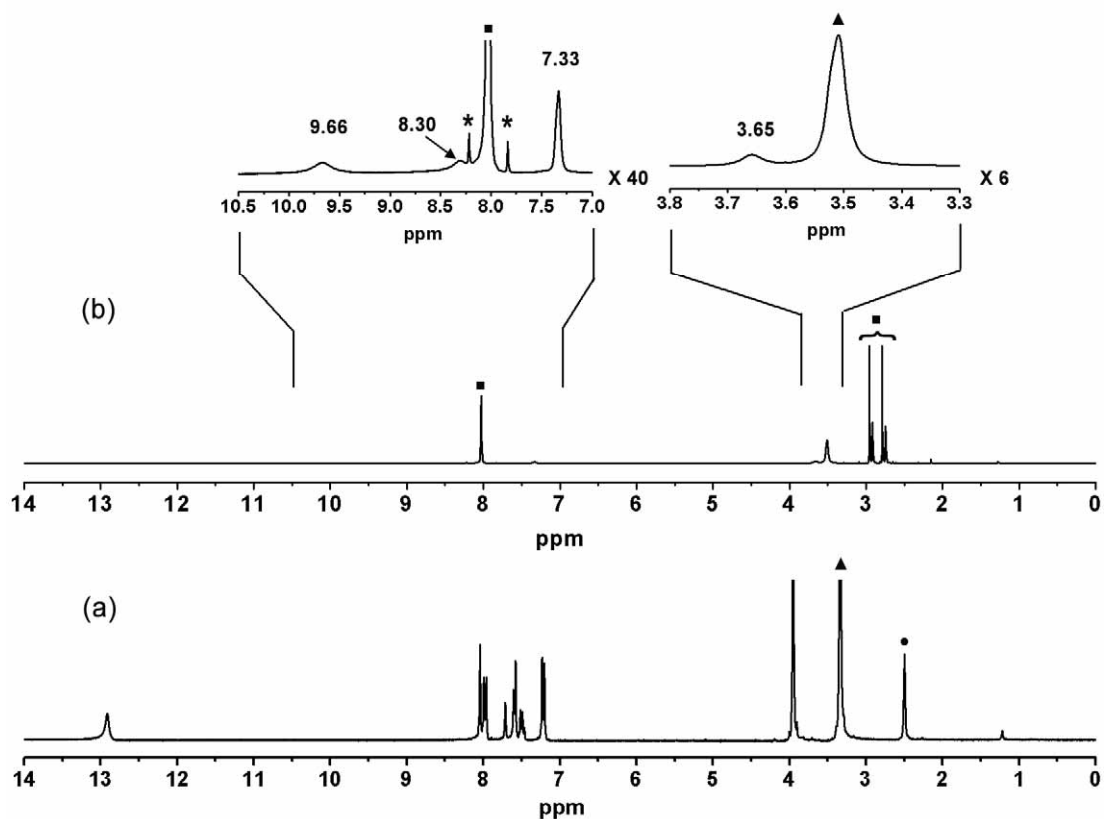


Figure S21. ¹H-NMR spectra of (A) H₂L² ligand in DMSO-*d*₆ and (B) MOP-2 in DMF-*d*₇. Symbols denote DMF (■), DMSO (●), and water (▲). The two spinning side bands of a proton peak of the solvent DMF at around 8 ppm are indicated with (*).

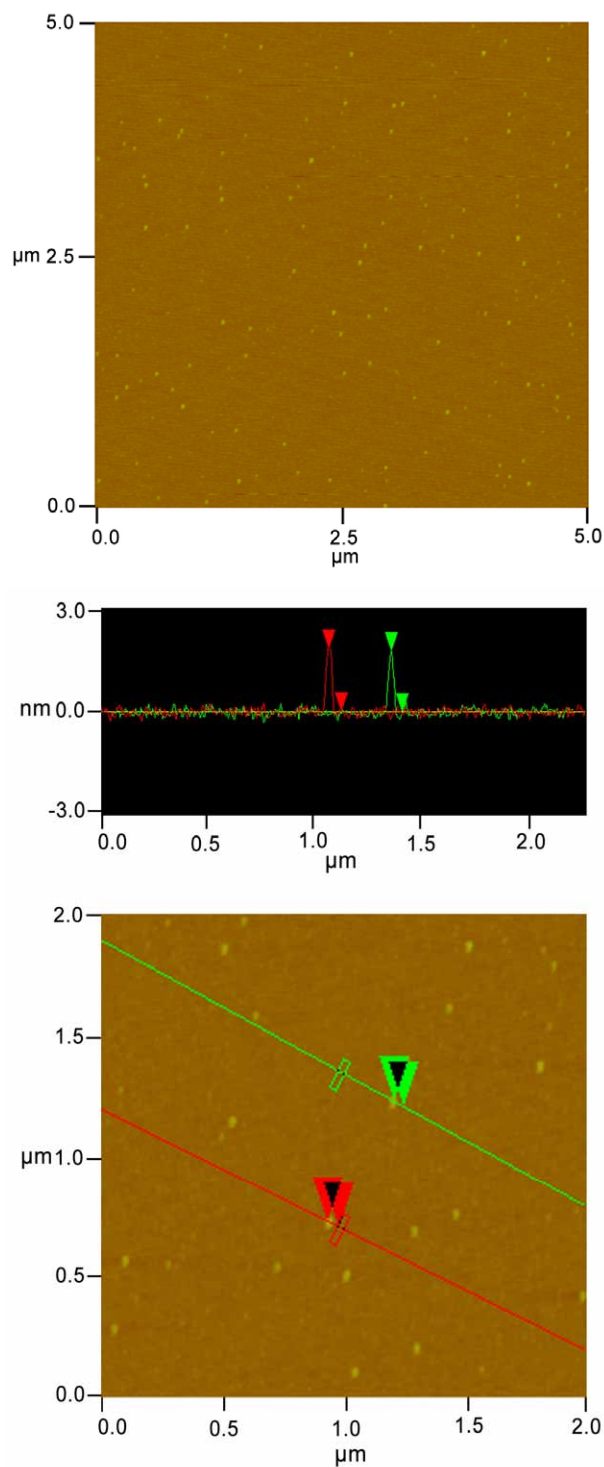


Figure S22 . (a) A typical AFM image of individual cages of MOP-2 on a mica surface with large magnification. (b) An enlarged AFM image of individual cages of MOP-2 (bottom), and the height profiles of some cages (top).